Evaluation of the Stress State in Aluminium Foam Sandwiches

Conference Paper · September 2010

DOI: 10.4203/ccp.93.276

4 authors:

F. Palano
ENEA

V. Dattoma

Riccardo Nobile
Università del Salento

F. W. Panella
Università del Salento

Proceedings of the Tenth International Conference
on Computational Structures Technology,
B.H.V. Topping, J.M. Adam, F.J. Pallarés,
R. Bru and M.L. Romero, (Editors),
Civil-Comp Press, Stirlingshire, Scotland

Paper 276

Evaluation of the Stress State in Aluminium Foam Sandwiches

F. Palano, V. Dattoma, R. Nobile and F.W. Panella
Department of Engineering for Innovation
University of Salento, Lecce, Italy

Abstract

In this paper a discussion about the determination of the stress state corresponding to the application of a four-point bending load on a sandwich panel having a core made of closed cell aluminium foam is reported.
An analytical model based on laminated plate classical theory is compared to a more complex FEM model, considering the effect of geometric parameters of panels, like core and plate thickness, and of loading mode, like span length.
The results show the difficulties to define a reliable model to calculate stress state in this kind of composite material.

Keywords: sandwich sheets, aluminium foam, four points bending, analytical model, finite element method.

1 Introduction

Sandwich sheets are employed in several industrial applications in which stiffness, strength and lightness properties are simultaneously considered essential.
Sandwich panels having metallic foam core [1-3] present numerous advantages with respect to honeycombs. In fact, they can be formed with integrated skins and easily moulded in curved shapes.
Recent advances in aluminium foam production processes and the shading in costs led new interest for this new class of materials, so that the possible employ in several fields such as aerospace, transportation (automotive, shipbuilding, railway) and building has been considered.
Metallic foams can be connected with dense metal skins during the foaming process or alternatively in a subsequent stage. These sandwich sheets are able to provide high performances under a bending load and to guarantee excellent lightness and stiffness.

This work analyses the four points bending behaviour of sandwich panels having foam core among the most representative available in commerce, highlighting particularly the geometric differences and sheets production effects on fatigue strength.
The aim of this work is to compare different models for the evaluation of stress state in aluminium foam sandwich panels subjected to four points bending, highlighting particularly the effects of distance between the supports and of core and plate thickness. Results have been compared to experimental data and to data available in scientific literature about mechanical behaviour of aluminium foam sandwich panels.
Sandwich panels that have been considered are characterised by these properties:

- plate thickness 1.2 and 1.7 mm
- overall thickness 20 and 32 mm
- sheet material EN AW 6060
- foam material AlSi6Cu6

A certain number of specimens having 200x80 mm dimension have been used to perform experimental static test in four point bending. Several arm distance between rollers in the range 25-60 mm have been also considered.
Some experimental data about static and fatigue behaviour of foams [4-10] and sandwich panels with foam core [11-16] can be traced in scientific literature.
A notable amount of information related to foams loading through four points bending is reported in Zettl and al. paper [9], in which the results obtained in different loading conditions are normalized with respect to the plateau stress σ_{pl}, in order to consider the foam density differences.
Results of experimental tests could be certainly reported in terms of applied bending, but the possibility of comparison among the different panels typologies would be lost. Particularly, it would be hard to establish what geometrical parameters have a relevant influence on foam sandwich strength.
For this reason, it is necessary to develop reliable models in order to estimate the stresses in the different layer forming the sandwich. The chance to apply laminated plate classical theory solution for determining state of plane stress of flat symmetric laminates is studied in [17].
The reliability of analytical model has been also confirmed by a numerical model of the different aluminium foam sandwiches. FEM analysis was performed using the Abaqus 6.9 software adopting a discretization in elements having 20 nodes and a quadratic reduced integration formulation.

2 Experimental tests

2.1 Materials

The tested specimens have been realized by means of a particular production process, since the faces and the core are connected by brazing. This aluminium foam sandwich with brazed skins are produced by Alm-GmbH and they are realized with

aluminium alloy EN AW 6060 skins (having thickness 1.2 and 1.7 mm) and AlSi6Cu6 core; they are thick in all 20 and 32 mm.
Detailed characteristics of the four AFS (Aluminium Foam Sandwich) panels are resumed in Table 1.

		AFS-1	**AFS-2**	**AFS-3**
Producer		Alm-GmbH	Alm-GmbH	Alm-GmbH
Panel thickness	**t [mm]**	20	32	20
Skins thickness	**t_s[mm]**	1.2	1.7	1.7
Foam core thickness	**t_f [mm]**	17.6	28.6	16.6
Skins material		EN AW 6060	EN AW 6060	EN AW 6060
Skins elastic modulus	**E_s [N/mm^2]**	67000	67000	67000
Skins density	**ρ_s [g/cm^3]**	2.70	2.70	2.70
Skins-core junction		brazing	brazing	brazing
Core material		AlSi6Cu6	AlSi6Cu6	AlSi6Cu6
Number of specimens		26	15	24

Table 1: Studied sandwiches characteristics.

The sandwich laminates, available in shape of panels with approximately sizes 500x500 mm, have been cut in order to achieve specimens having plan dimensions 200x80 mm. A total number of 65 specimens has been tested.
These samples have been employed in four points bending fatigue tests.
The support distance value has been selected in the range 25÷60 mm in dependence on testing machine loading capacity. However, it has been verified that support distance variation in this gap does not influence either the strength or the failure mode.

2.2 Failure mode

Possible failure modes which characterised laminates with foam core are face-skin yield, core shear and core indentation (Figure 1). Failure mechanism derives from geometric parameters, loading conditions and foam strength; important factors for failure mode are also the core and skins thickness, the distance between the supports and the relative fatigue strength of face sheets to core. All these parameters, opportunely valued, allowed to get failure maps definition [16]; from the examination of the geometric characteristics and the testing system, a failure mode due to foam core shear is expected, according to what reported in Figure 1. The hypothesis has been effectively confirmed by the realized experimental tests. This failure mode can be considered the most common in AFS panels employment standard conditions [16].

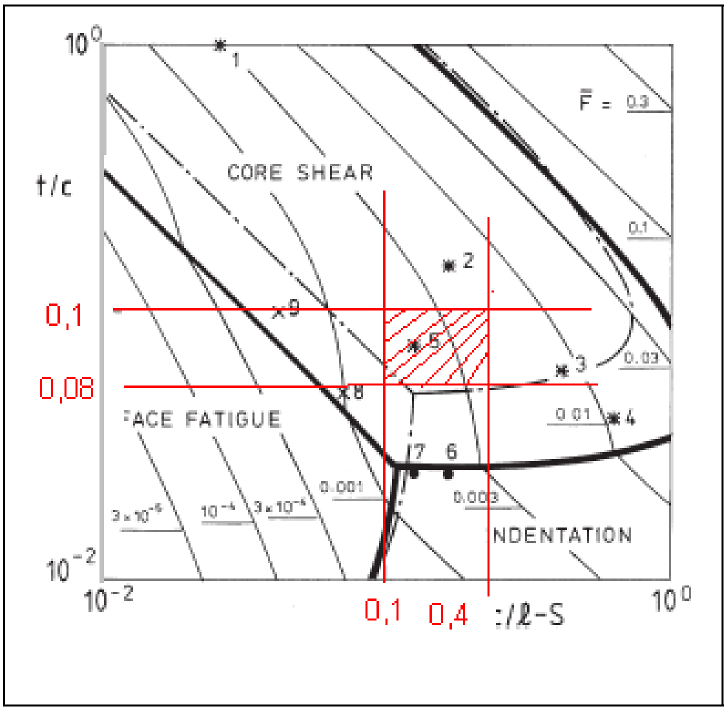

Figure 1: Failure mode determination.

In fact, failure mode of examined sandwiches is mostly due to foam core shear yielding (Figure 2).

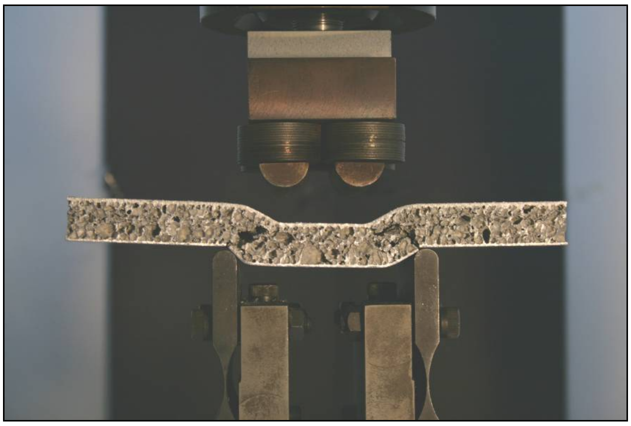

Figure 2: Failure mode for AFS-1 specimen.

During fatigue test, the specimens stiffness remains practically constant, while in previous experiments it was noticed that samples formed only by foam showed a progressive deformation [10].
Shear stress, which is higher near the laminate middle line, induces little micro-fractures randomly oriented caused by material in-homogeneity. These micro-fractures number and dimension increase till a complete horizontal crack formation. The phenomenon is accompanied by stiffness reduction and some material quantities expulsion. The horizontal crack grows up rather quickly at first in horizontal

direction and then diagonally, until it reaches the external skins faces (Figure 3). It is not assured that the crack is externally visible, since it can develop in the central zone of the specimen. Initial fracture length is observed to be strongly influenced by supports distance, while the number of cycles to failure does not vary according to it.

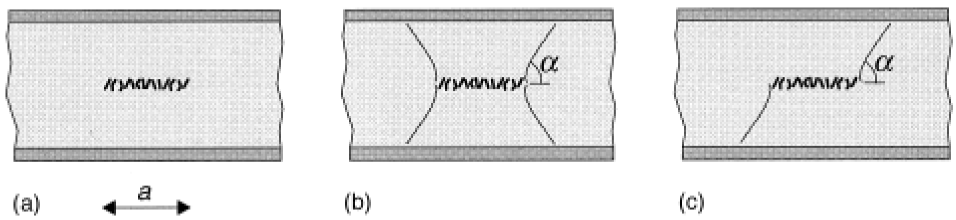

Figure 3: Failure phases: a) horizontal crack formation ; b) inclined propagation; c) propagation up to external skins.

Final breaking, which interests also external skins, can take place in several ways and it is conditioned by shear force entity: for thickness lower than 20 mm a plastic skins yielding (Figure 3a) or more rarely the skin breaking (Figure 3b) can occur; for thickness higher than 32 mm, corresponding to AFS-2 series specimens, which are loaded with greater shear stresses, the failure happens as skin total fracture or more often for skin detachment by core (Figure 3c).

3 Analytical model

Tests results can certainly be reported as outer bending moment, but in this way the possibility of objective confront among the four panels typologies would be lost. Particularly, it would be hard to establish if mechanical strength is dependent on sandwich total thickness or skins thickness.
For this reason, it is necessary to employ an analytical model in order to estimate the stresses in different layers forming the sandwich. The chance to apply laminated plate classical theory solution for determining plane stress state of flat symmetric laminates is studied in [17].
Based on what here reported, exact elastic solution is well approximated by laminated plate classical theory for tensional state determination, but it undervalues considerably the displacements effects. Furthermore, approximation improves if sheet width/thickness ratio increases.
In the examined case, this ratio is included between 2.5 and 4 for specimens having 32 and 20 mm thickness respectively, however guarantying a sufficient approximation especially for the tensional field.
For this reason, maximum bending stress in foam and skins layers will be evaluated with the following formulas:

$$\sigma_{foam} = \frac{TE_f}{(EJ)_{eq}} \frac{t_f}{2} \tag{1}$$

$$\sigma_{skin} = \frac{TE_s}{(EJ)_{eq}} \frac{t_s}{2} \tag{2}$$

with:

$$\left(EJ\right)_{eq} = b\left[\frac{1}{12}t_f^3 E_f + \frac{1}{6}t_s^3 E_s + 2E_s t_s \left(\frac{t_f}{2} + \frac{t_s}{2}\right)^2\right] \tag{3}$$

in which:
- E_f, Es: foam and skin material Young's modulus, respectively;
- t_f, ts, e t: foam, skins and sheet thickness, respectively.

4 Numerical analysis

A numerical model was realized in order to verify if the laminated plate classical theory could be really applied on AFS panels to be tested.
Pagano affirmed in his work [17] that this theory can be applied on composites for width/thickness ratio (S=a/h) greater than 4, since only for these S values it approaches the experimental results.
FEM analysis was performed using the Abaqus 6.9 software adopting a discretization in elements named C3D20R, having 20 nodes and a quadratic reduced integration formulation (Figure 4).
Boundary conditions were applied on the lower face, imposing a zero value to z-direction displacement; pressure load was applied to nodes on the upper surface and it was set accordingly to the AFS typology and supports distance (Figure 5). Geometric non-linearity effects have been considered using large displacements option.

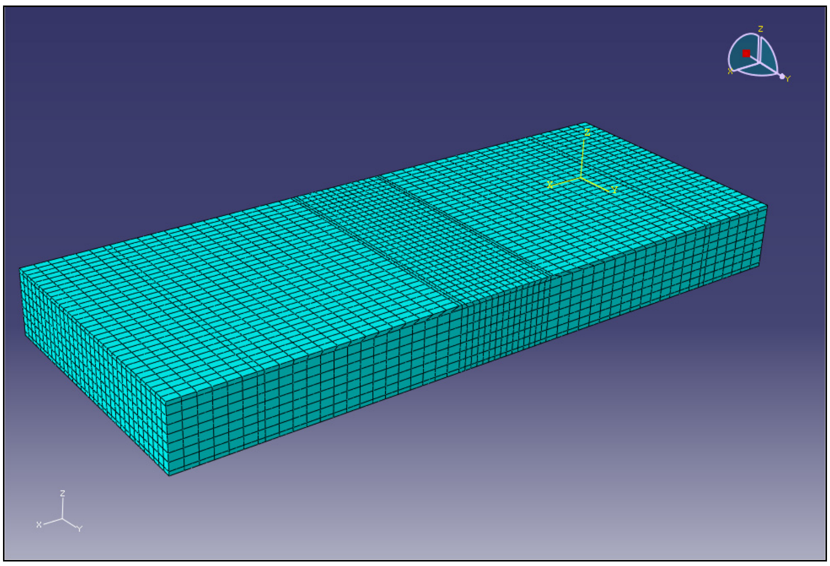

Figure 4: Mesh realized on the FEM model.

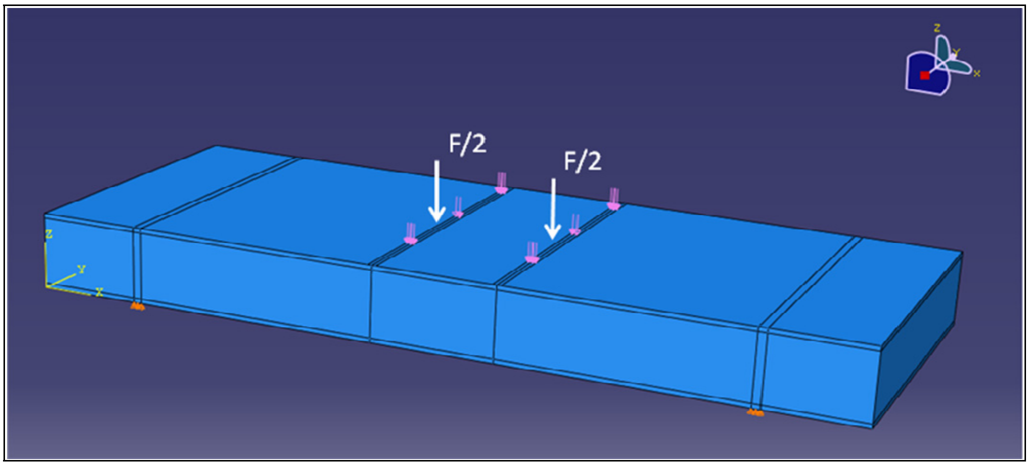

Figure 5: Loads and boundaries applied to the AFS model.

The simplest model considered an isotropic elastic behaviour both for aluminium plate and foam. The material model was isotropic with elastic behaviour, using skins and foam properties summarised in Table 2 and Table 3 respectively.

Skin	**Density [g/cm^3]**	**Yielding Stress [N/mm^2]**	**E [N/mm^2]**
EN AW 6060	2.7	276	67000

Table 2: skins mechanical characteristics [19].

Foam	**Density [g/cm^3]**	**Plateau stress [N/mm^2]**	**$E_{loading}$ [N/mm^2]**	**$E_{unloading}$ [N/mm^2]**
AlSi6Cu6	0.32	3.82	105.7	475

Table 3: foam mechanical characteristics.

The material properties, reported in Table 3, were the actual mechanical properties measured directly on Alm-GmbH foam by mechanical characterisation. The apparent density was assumed equal to the actual density of the foam, about 320 kg/m^3 [18].
Foam macroscopic bending stress σ_{11}, Von Mises stress and compression stress σ_{33} were calculated and recorded at each load increment.
Since bending is the preponderant stress in the applied loading condition, a bi-triangular stress trend is expected. Instead, the σ_{11} plot does not show a symmetrical bi-triangular diagram (Figure 6). This situation is probably due to a tri-axial stress state acting in the sandwich. In fact, the compression stress σ_{33} presents the same magnitude of the bending stress σ_{11} (Figure 7).
Therefore, the application of laminated plate classical theory to AFS could be acceptable also for S smaller than 4, but only with some corrections, since the bending stress and the compressive one have the same magnitude orders. Due to this fact, the bending stress, even if it has a butterfly pattern, results to be not symmetric with respect to the geometric neutral axis (Figure 6).

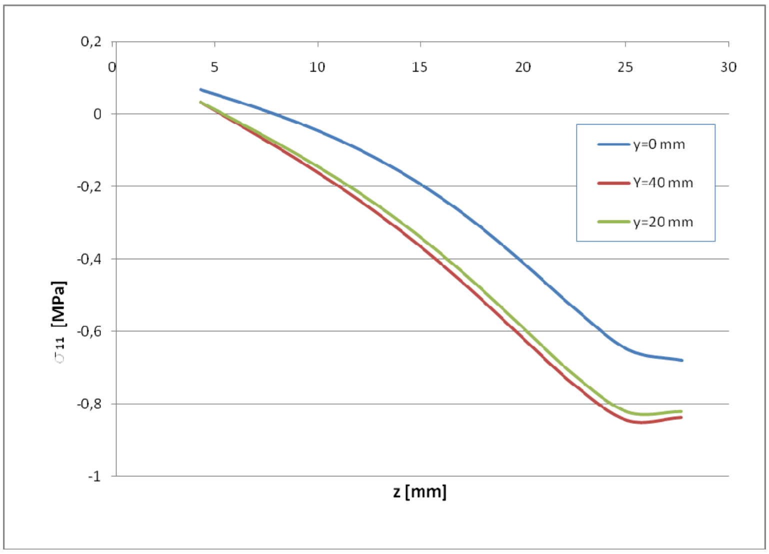

Figure 6: Foam core σ_{11} trend versus z axis (thickness) at the middle of the x axis considered in three different positions along the y axis.

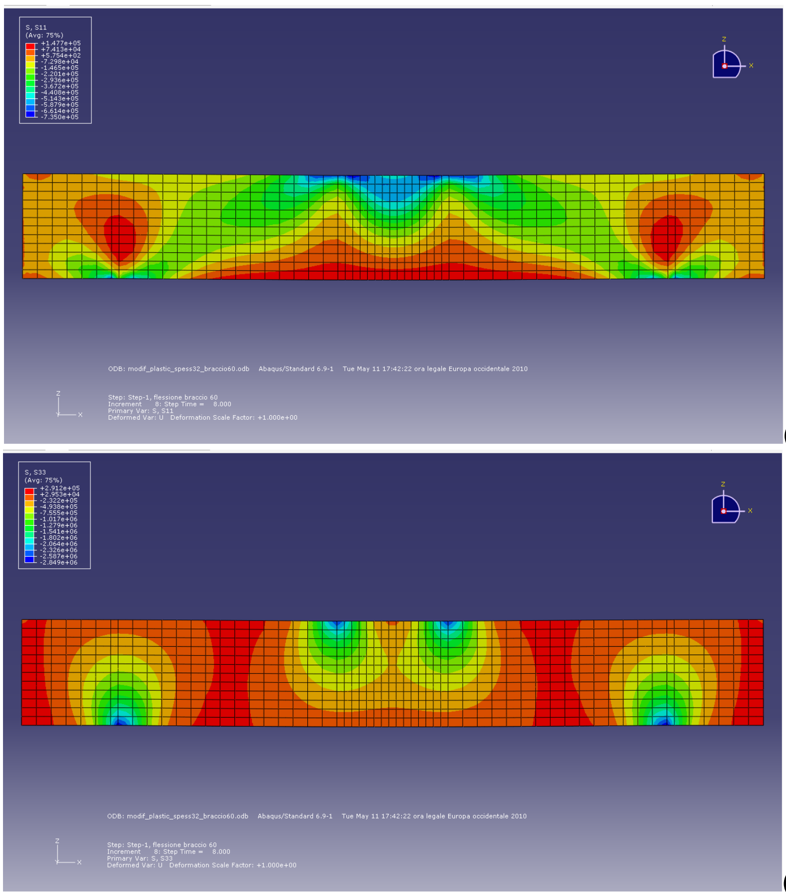

(a)

(b)

Figure 7: σ_{11} (a) and σ_{33} (b) pattern in the middle of the width for AFS-2 tested with arm 60 mm.

A comparison between numerical and analytical results calculated for each AFS geometry and loading configuration showed that the maximum stress values are localised in the core–skin interface.
Data deduced by numerical simulations and those analytically calculated on the base of the experimental tests have been compared for each AFS typology.
In the following tables, the maximum stress values, those corresponding to core–skin interface, are considered for each geometry and for each applied load F.
A comparison of results are reported in the following tables and they are expressed in terms of maximum stress.

Arm [mm]	F [N]	σ_{11} analytic [MPa]	Elastic model		Plastic model	
			σ_{VM} numerical [MPa]	σ_{11} numerical [MPa]	σ_{VM} numerical [MPa]	σ_{11} numerical [MPa]
25	1400	0.07	0.04	0.04	0.03	0.04
	2200	0.11	0.06	0.06	0.05	0.07
	2850	0.15	0.07	0.08	0.07	0.08
	2400	0.13	0.06	0.07	0.06	0.07
	2750	0.14	0.07	0.08	0.07	0.08
	4000	0.21	0.10	0.12	0.10	0.12
	3000	0.16	0.08	0.09	0.08	0.09
	2800	0.15	0.07	0.08	0.07	0.08
	2900	0.15	0.07	0.08	0.07	0.09
	3100	0.16	0.08	0.09	0.08	0.09
	3200	0.17	0.08	0.0.9	0.08	0.10
	3300	0.17	0.08	0.10	0.08	0.10
	3400	0.18	0.09	0.10	0.09	0.10
	3500	0.18	0.09	0.10	0.09	0.10
40	2000	0.16	0.03	0.03	0.02	0.03
	1900	0.17	0.02	0.03	0.02	0.03
	1800	0.15	0.02	0.03	0.02	0.03
	2200	0.18	0.03	0.03	0.03	0.03
	1700	0.14	0.02	0.03	0.02	0.03
	1800	0.15	0.02	0.02	0.02	0.03
	2100	0.17	0.03	0.03	0.03	0.03
60	1500	0.18	0.04	0.02	0.04	0.02
	1600	0.2	0.05	0.03	0.04	0.02
	1550	0.19	0.04	0.02	0.04	0.02
	1450	0.18	0.04	0.02	0.04	0.02
	1400	0.17	0.04	0.02	0.04	0.02
	1350	0.17	0.04	0.02	0.04	0.02

Table 4: Comparison between numerical and analytical data for AFS-1 panels.

In a second time, elasto-plastic isotropic hardening and crushable foam models have been used for skins and core respectively.
The skins utilized a bilinear constitutive model with the following characteristics [19]:

- density 2700 kg/m^3
- elastic modulus 67000 MPa
- Poisson's ratio 0.33
- Yielding stress: 210 MPa
- Plastic modulus: 293 MPa

For aluminium foam the crushable foam available in Abaqus has been chosen, adopting the following base material characteristics [18]:

- density 320 kg/m^3
- elastic modulus 475 MPa
- Poisson's ratio 0.3
- compression yield stress ratio 1.5
- zero plastic Poisson's ratio
- isotropic crushable foam hardening
- yielding stress 3.82 MPa
- zero uniaxial plastic strain

Arm [mm]	**F [N]**	**σ_{11} analytic [MPa]**	**Elastic model**		**Plastic model**	
			σ_{VM} numerical [MPa]	**σ_{11} numerical [MPa]**	**σ_{VM} numerical [MPa]**	**σ_{11} numerical [MPa]**
40	6000	0.19	0.15	0.06	0.17	0.02
	6300	0.20	0.15	0.06	0.18	0.02
	6600	0.21	0.16	0.07	0.19	0.02
	6900	0.22	0.17	0.07	0.20	0.03
	7500	0.23	0.18	0.07	0.22	0.03
	8000	0.25	0.20	0.08	0.23	0.03
	7300	0.23	0.18	0.07	0.21	0.03
	4500	0.14	0.11	0.04	0.13	0.02
60	5300	0.24	0.22	0.07	0.21	0.06
	4800	0.22	0.20	0.06	0.19	0.06
	4000	0.19	0.16	0.05	0.16	0.05
	4300	0.20	0.18	0.06	0.17	0.05
	4200	0.19	0.17	0.05	0.17	0.05
	4400	0.21	0.18	0.06	0.18	0.05
	4600	0.21	0.19	0.06	0.18	0.05
	5200	0.24	0.21	0.07	0.21	0.06
	4100	0.19	0.17	0.05	0.16	0.05

Table 5: Comparison between numerical and analytical data for AFS-2 panels.

Arm [mm]	F [N]	σ_{11} analytic [MPa]	Elastic model		Plastic model	
			σ_{VM} numerical [MPa]	σ_{11} numerical [MPa]	σ_{VM} numerical [MPa]	σ_{11} numerical [MPa]
25	2600	0.08	0.04	0.07	0.04	0.07
	4800	0.15	0.07	0.12	0.08	0.12
	3500	0.11	0.05	0.09	0.06	0.09
	3600	0.12	0.06	0.09	0.06	0.09
	3700	0.12	0.06	0.09	0.06	0.10
	4000	0.13	0.06	0.10	0.06	0.10
	3900	0.13	0.06	0.10	0.06	0.10
	4100	0.13	0.06	0.10	0.07	0.11
	4500	0.14	0.07	0.11	0.07	0.12
40	2700	0.14	0.02	0.04	0.02	0.04
	3000	0.16	0.02	0.04	0.02	0.04
	3100	0.16	0.02	0.04	0.02	0.04
	2800	0.14	0.02	0.04	0.02	0.04
	2900	0.15	0.02	0.04	0.02	0.04
	3200	0.16	0.03	0.04	0.03	0.04
	2600	0.13	0.02	0.03	0.02	0.04
	3300	0.17	0.03	0.04	0.03	0.05
60	3000	0.23	0.07	0.07	0.07	0.03
	2900	0.22	0.07	0.07	0.06	0.03
	2800	0.22	0.06	0.07	0.06	0.02
	2700	0.21	0.06	0.07	0.06	0.02
	2600	0.21	0.06	0.06	0.06	0.02
	2200	0.17	0.05	0.05	0.05	0.02
	2400	0.19	0.05	0.06	0.05	0.02
	2000	0.16	0.05	0.05	0.04	0.02

Table 6: Comparison between numerical and analytical data for AFS-3 panels.

From the previous tables, it is evident that the analytical σ_{11} stress is always greater (sometimes a lot) than that numerically evaluated. The difference between the bending stress is bigger as span length increases.

From the numerical model the stress state does not result uniaxial. Particularly, the compression stress derived from the load application is not negligible. Then, it is suitable to use as reference σ_{VM} instead of σ_{11}.

The difference between σ_{11} and σ_{VM} is mostly evident for AFS-2 sandwiches (Table 5), in which the core has a larger thickness. Compressive stress in the core, in fact, is strongly predominant respect to bending component, since the foam presents an elastic modulus clearly lower than the aluminium alloy skins one.

Better results of laminated plate classical theory are obtained especially for AFS characterised by a small foam/skin thickness ratio, since compression effect in the foam is increased in case of large foam thickness (AFS-2). In this case there is coherence between the analytical data and the Von Mises stress computed by the numerical model. Moreover, Von Mises stress in the foam core follows the failure mode lines experimentally verified (Figures 8 and 9).

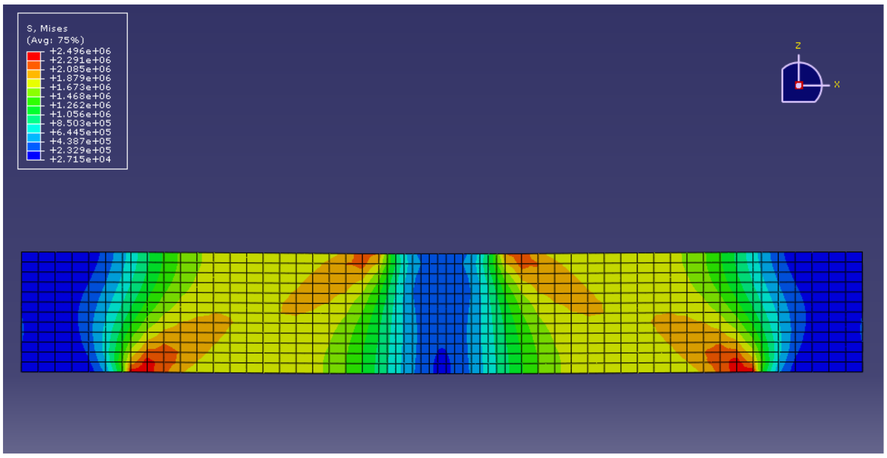

Figure 8: Elastic model - Von Mises stress pattern for AFS-2 tested with arm 60 mm.

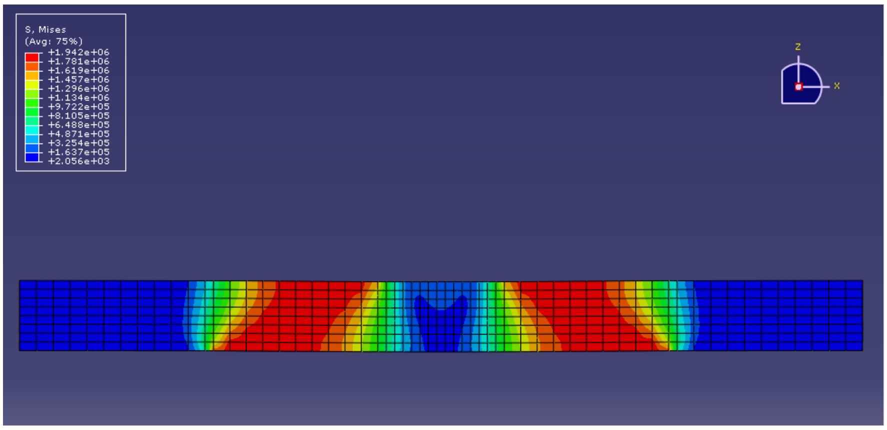

Figure 9: Elastic model - Von Mises stress pattern for AFS-3 tested with arm 40 mm.

For AFS-3 panels the bending stress is prevalent respect to the compression one.
So, it seems to be greater accordance between σ_{11} values obtained trough analytical and numerical model.
For AFS-1 panels, σ_{11} is always predominant, but the difference between σ_{11} and σ_{33} is smaller respect to the other AFS typology, since the foam/skin thickness ratio is greater (Table 4). So, in this case, major accordance seems to be between analytical results and Von Mises stress data.

In conclusion, in order to establish if it is more correct to adopt Von Mises stress or bending stress σ_{11} evaluate analytically, we must consider the foam/skin thickness ratio, since compression is greater in foam core, while bending in the aluminium alloy skins.
However, the results for all the samples having smaller thickness (AFS-1 and AFS-3 sheets) show that the approximation of analytic stress with the bending one calculated from the numerical model is not wrong.
From the Tables 4-6 it is evident that numerical simulations with plastic materials or with elastic materials give practically the same results.
For AFS panels having thickness 20 mm (AFS-1 and AFS-3), which have thinner foam thickness, the analytical computed stress is similar to numerically evaluated bending stress σ_{11} (Tables 4 and 6). This result is not always true for AFS-3 panels, which have greater skins thickness (1,7 mm).
Von Mises stress distributions for all AFS kinds are shown in the following figures (Figures 10-12): there is coherence between analytical data and Von Mises stress computed by the numerical model.
This confirmed the failure maps conclusions reported in Figure 1 and especially the failure mode (shear) revealed during the experimental tests carried out.

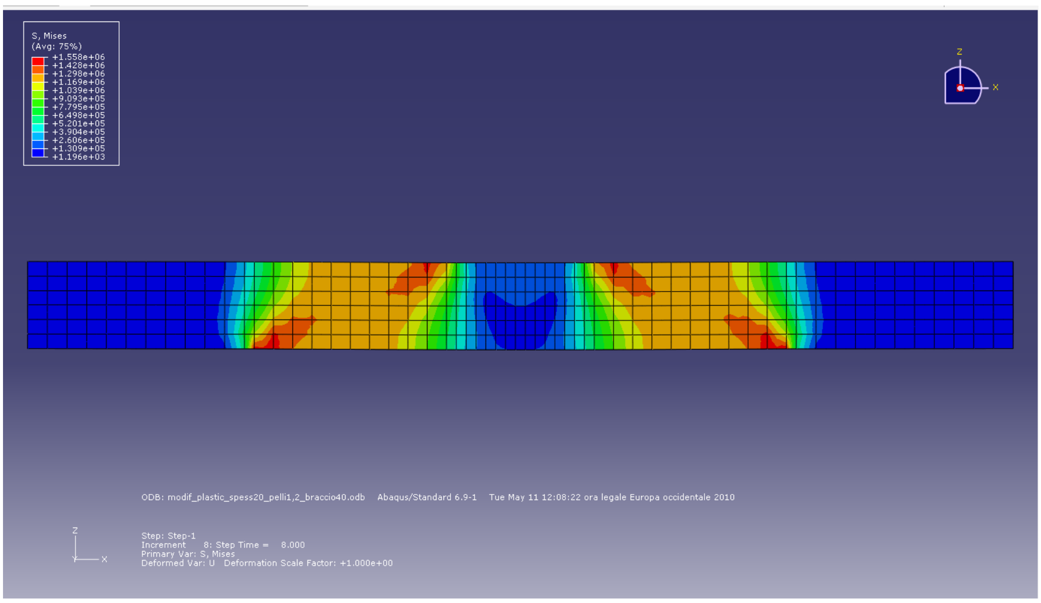

Figure 10: Plastic model - Von Mises stress pattern for AFS-1 tested with arm 40 mm.

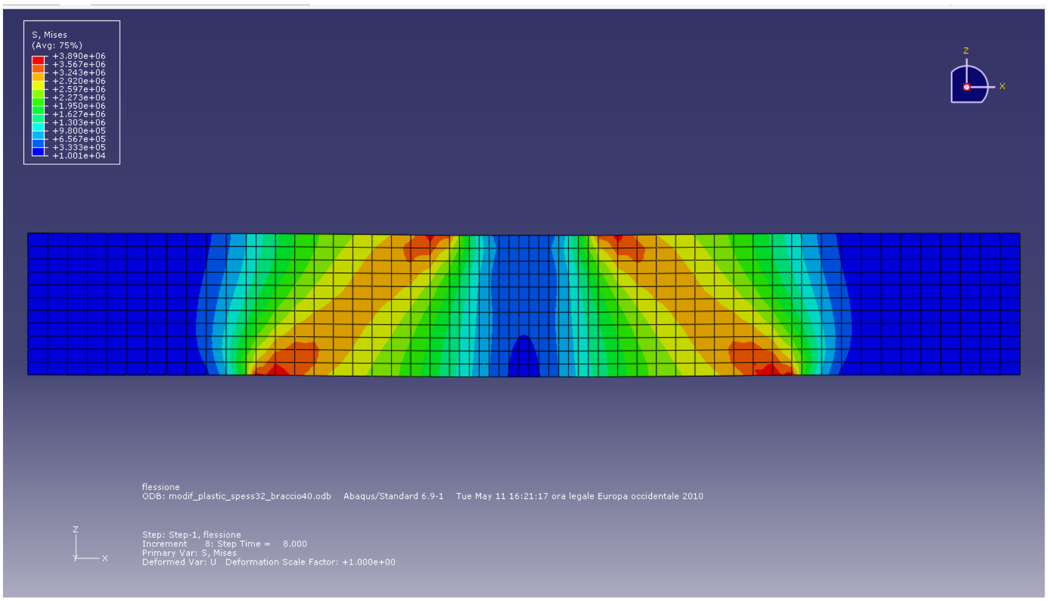

Figure 11: Plastic model - Von Mises stress pattern for AFS-2 tested with arm 40 mm.

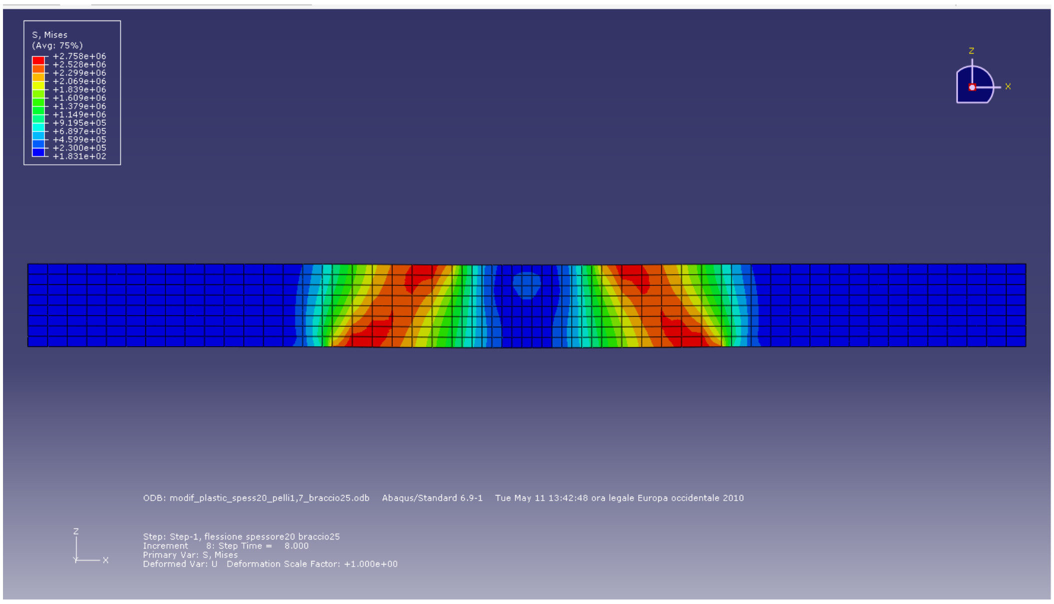

Figure 12: Plastic model - Von Mises stress pattern for AFS-3 tested with arm 25 mm.

5 Conclusions

Mechanical characterization of sandwich laminates formed by aluminium alloy skins and foam core has been realized on three sandwich typologies, chosen among the

most representative available in commerce. The three sandwich sheets are different for skins and core thickness.
Computation of stresses applied in the mechanical tests has been realized with a simple analytical model based on laminated plate classical theory and a numerical FEM model.
The stress assumed as reference is core stress localised in the core–skin interface, which appears the most representative between the possible tensional parameters.
Failure mode is ruled by shear foam core collapse and it is dissimilar in the final step for laminates having different thickness, due to applied shear force entity.
Values of maximum stress calculated by analytical and numerical models are highly different. In particular, analytical model gives stress that are generally 2-3 time higher than those calculated by numerical model. However, analytical model, in which bending is the only acting stress, is often not acceptable since compressive stress due to local application of the load has generally the same magnitude of bending stress. For this reason, it is more appropriated to consider a Von Mises equivalent stress rather than the bending stress to describe the stress state in the foam.
Finally, the use of more adequate constitutive models for aluminium plate skin and aluminium foam does not change significantly stress results and constitutes an useless complication of the model.

References

[1] M.F. Ashby, A.G. Evans, N.A. Fleck, L.J. Gibson, J.W. Hutchinson, H.N.G. Wadley, "Metal Foams: A Design Guide", Butterworth-Heinemann publications, 2000.

[2] J.Banhart, "Manufacture, characterization and application of cellular metals and metal foams", Progress in Materials Science, 46, 559-632, 2001.

[3] V. Dattoma, R. Nobile, F.W. Panella, R. Tafuro, "Comportamento meccanico di pannelli sandwich in schiuma di alluminio", Atti del XXXIV Convegno nazionale AIAS, Politecnico di Milano, 14 -17 settembre 2005.

[4] E. Andrews, W. Sanders, L.J. Gibson, "Compressive and tensile behaviour of aluminium foams", Materials Science and Engineering A, 270, 1999.

[5] E. Guglielmino, R. Montanini, "Caratterizzazione sperimentale di schiume metalliche in alluminio", Atti del XXXI Convegno Nazionale AIAS, Parma, 18-21 settembre 2002.

[6] G. B. Broggiato, F. Campana, G. Santucci, "Analisi sperimentale del comportamento di schiume d'alluminio", XXX Convegno nazionale AIAS, Alghero (SS), 12-15 Settembre 2001.

[7] J. Banhart, J. Baumeister, "Deformation characteristics of metal foam", Joumal of Materials Science, 33, 1431-1440, 1998.

[8] J. Banhart, W Brinkers, "Fatigue behaviour of aluminium foams", Journal of materials science letters, 18, 617-619,1999.

[9] B. Zettl, H. Mayer, S.E. Stanzl-Tschegg , H.P. Degischer, “Fatigue properties of aluminium foams at high numbers of cycles”, Materials Science Engineering, 2000 (1-7).
[10] V. Dattoma, N.I. Giannoccaro, A. Messina, R. Nobile, “Fatigue damage evaluation of metallic foam specimens through modal data”, SEM XI International Conference of Society of Experimental Mechanics, Orlando Florida (USA), 2-5 June 2008.
[11] A.M. Harte, N.A. Fleck, M.F. Ashby, “Sandwich panel design using Aluminium alloy foam”, Advanced Engineering Materials, 4, 219-222, 2000.
[12] C. Chen, A-M Harte, N.A. Fleck, “The plastic collapse of sandwich beams with a metallic foam core”, International Journal of Mechanical Sciences, 43, 1483-1506, 2001.
[13] O. Kesler, L. J. Gibson, “Size effects in metallic foam core sandwich beams”, Materials Science and Engineering, A326, 228-234, 2002.
[14] H. Barth-Smith, J.W. Hutchinson, N,A. Fleck, A.G. Evans, “Influence of imperfections on the performance of metal foam core sandwich panels”, International Journal of Solids and Structures, 39, 4999-5012, 2002.
[15] M. Burman, D. Zenkert, “Fatigue of foam core sandwich beams”, International Journal of Fatigue, 7, 551-561, 1997.
[16] A.M. Harte, N.A. Fleck, M.F. Ashby, “The fatigue strength of sandwich beams with an aluminium alloy foam core”, International Journal of Fatigue, 23, 499-507, 2001.
[17] N.J. Pagano, “Exact solutions for rectangular bidirectional composites and sandwich plates”, Journal of Composite Materials, 4, 20-34, 1970.
[18] V. Dattoma, R. Nobile, F. Palano, F.W. Panella, “Comportamento a fatica di pannelli sandwich in schiuma di alluminio”, XXXVII Convegno AIAS, Roma, 10-13 settembre 2008.
[19] ASM Metals Handbook, vol. 2, “Properties and selection: non-ferrous alloys and special-purpose materials”, 10^{th} edition, ASM International, 1993.